Ossietzky Universität Oldenburg, Oldenburg, Germany, 1994), pp. 97–105; F. Pflüger, *Neues. Jahrb. Geol. Palaeontol. Abh.* **195**, 75 (1995).
10. A. Seilacher, *Fossil Art* (Royal Tyrell Museum of Paleontology, Drumheller, Alberta, Canada, 1997).
11. ———, *Geol. Soc. Am. Abstr. Progr.* **32**, 193 (1997).
12. J. G. Gehling, *Mem. Geol. Surv. India* **20**, 181 (1991).
13. H. J. Hofmann, *Bull. Geol. Surv. Canada* **189**, 146 (1971).
14. S. Sarkar, S. Banerjee, P. K. Bose, *Neues Jahrb. Geol. Palaeontol. Monatsh.* **7**, 432 (1996).
15. The corrugated structures from the Koldaha Shales (*14*) may well be impressions of segmented algae (A. H. Knoll, personal communication).
16. A. P. Vinogradov *et al.*, in *Absolyutnoye Datirovanie. Tektono-Magmaticheskih Siklovi Etapov ordeneriya po dannim 1964* (Nauka, Moscow, 1966).
17. A. P. Srivastava and G. Rajagopalan, *J. Geol. Surv. India* **32**, 527 (1988).
18. A. I. Tugarinov, L. L. Shanin, G. A. Kazakov, M. M. Arakelyanta, *Geokhimiya* **6**, 652 (1965).
19. A. P. Vinogradov and A. I. Tugarinov, *Proc. Int. Geol. Congr.* **10**, 652 (1964).
20. G. Rajagopalan and P. K. Maithy, *Group Discussion on Vindhyans* (Jadavpur University, Calcutta, 1993), pp. 35–36.
21. A. P. Srivastava and G. Rajagopalan, in *Nuclear Tracts*, K. K. Sharma, Ed. (Government of India, New Delhi, 1986), pp. 41–52.
22. A. P. Srivastava, G. Rajagopalan, K. K. Nagpaul, *Indian J. Earth Sci.* **12**, 89 (1985).
23. Trips to India were made possible by the Crafoord Prize (1992) of the Swedish Academy and through support by Coy Squires (Houston). We also thank E. Klitzsch, H. Luginsland, S. Sarkar, and E. Seilacher for assistance in the field. Photographs were taken by W. Gerber (Fig. 3) and W. Sacco (Fig. 2), and word processing was completed by E. Seilacher.

24 April 1998; accepted 29 July 1998

ROSAT X-ray Detection of a Young Brown Dwarf in the Chamaeleon I Dark Cloud

Ralph Neuhäuser and Fernando Comerón

Photometry and spectroscopy of the object Cha Hα 1, located in the Chamaeleon I star-forming cloud, show that it is a $\sim10^6$-year-old brown dwarf with spectral type M7.5 to M8 and 0.04 ± 0.01 solar masses. Quiescent x-ray emission was detected in a 36-kilosecond observation with 31.4 ± 7.7 x-ray photons, obtained with the Röntgen Satellite (ROSAT), with 9σ detection significance. This corresponds to an x-ray luminosity of 2.57×10^{28} ergs per second and an x-ray to bolometric luminosity ratio of $10^{-3.44}$. These are typical values for late M-type stars. Because the interior of brown dwarfs may be similar to that of convective late-type stars, which are well-known x-ray sources, x-ray emission from brown dwarfs may indicate magnetic activity.

A brown dwarf (BD) is an object with a mass ≤ 0.08 solar masses ($M_\odot$), which is insufficient to sustain nuclear fusion of hydrogen (*1*). Lacking this source of energy against self-gravity, which provides the long-term stability of main-sequence stars, a BD shrinks in size until electron degeneracy halts further contraction. Because a BD becomes cooler and less luminous with age (*2*), some BD searches in the nearby (~125 pc) and young (~10^8 years) Pleiades cluster were successful (*3*). In ρ Ophiuchi (ρ Oph), a region with ongoing star formation, several low-mass objects were identified (*4*), including the object ρ Oph 1623-2426, a 3 to 10 × 10^6 year old BD (*5*). Stellar evolution theory predicts that stars with masses ≤ 0.3 $M_\odot$ are fully convective (*6*). Given the central role of convection for magnetic activity and x-ray emission in low-mass stars, a BD may emit x-rays by the same mechanism as low-mass stars. However, until now, no BD has been detected in x-rays.

In a survey of the Chamaeleon (Cha) I dark cloud, near-infrared (NIR) photometry and low-resolution, low signal-to-noise ratio (S/N) spectroscopy were obtained for several new faint cloud members (*7*), so that objects 1 to 6 [table 4 of (*7*)], called Cha Hα 1 to 6 here, all showing Hα emission lines in their spectra, could be plotted in the Hertzsprung-Russell diagram, assuming 160 pc as distance, which is the mean of the distances of three T Tauri stars in Cha I measured by Hipparcos, and a spectral type to temperature conversion for cool stellar photospheres (*8*, *9*). According to pre–main-sequence evolutionary tracks (*10*), these six objects are near and some are possibly below the stellar mass limit of 0.08 $M_\odot$.

After identifying these BD candidates, we retrieved the ROSAT pointed observations 200207 (31 ks) and 200046 (5 ks) from the ROSAT data archive. Both observations are centered on the Cha I cloud and were obtained in 1991 with the ROSAT Positional Sensitive Proportional Counter (PSPC) (*11*). We performed standard source detection with the Extended Scientific Analysis Software to reduce the merged data set (Fig. 1). Because of the ROSAT boresight offset, a few arc seconds offset can be allowed between the x-ray and the optical positions for source identification.

The object Cha Hα 1 is identified with the x-ray point source RXJ 110716-773552, whereas Cha Hα 3 and Cha Hα 6 are marginally detected. There are no other objects from SIMBAD, the Hubble Space Telescope Guide Star Catalog, or the NASA Extragalactic Database within 80 arc sec around these x-ray sources. None of these objects were detected in a less sensitive Einstein Observatory x-ray image of the same region (*12*). They were also not detected in an earlier analysis of the 5-ks PSPC pointing (*13*). However, Cha Hα 1 was detected in an earlier analysis of the 31-ks PSPC pointing, object XP 30 in (*14*), and it was tentatively identified as a faint stellar object of unknown class (*14*).

Given the spectral resolution of the PSPC, one can define several energy bands and calculate the so-called hardness ratios of detected x-ray sources. If $Z[a, b]$ is the count rate between energies a and b, then hardness ratios are defined as

$$HR1 = \frac{Z[0.5, 2.1] - Z[0.1, 0.4]}{Z[0.5, 2.1] + Z[0.1, 0.4]}$$

$$HR2 = \frac{Z[0.9, 2.1] - Z[0.5, 0.9]}{Z[0.9, 2.1] + Z[0.5, 0.9]}$$

To obtain x-ray fluxes for the detected objects as well as x-ray upper limits for undetected objects (Table 1), the count rates have to be divided by the appropriate energy conversion factor, namely, 10^{11} counts cm^{-2} erg^{-1}.

Because Cha Hα 1 is detected in the x-ray observation and because it is a good BD candidate in view of the previous data (*7*), we obtained low-resolution, high S/N spectra of this object with the 3.5-m New Technology Telescope (NTT) of the European Southern Observatory (ESO) on La Silla, Chile, in the visible [using the ESO Multi-Mode Instrument (EMMI), with resolution of ~1250 at 800 nm] and the NIR [using Son of Isaak (SOFI), an infrared spectrometer and array camera, with resolution of ~500 at 2 μm] in May 1998.

Both spectra (Fig. 2) show features typical of cool photospheres (≤3000 K). Most prominent in the visible is the Hα emission line with an equivalent width of 6.5 nm and many TiO and VO absorption lines. In the NIR, the CO absorption lines and the broad depression between 1.5 and 2.0 μm due to H_2O absorption also suggest a temperature below 2000 K. The strength of the gravity-sensitive Na I absorption feature at 819 nm is intermediate

R. Neuhäuser, Max-Planck-Institut für Extraterrestrische Physik, D-85740 Garching, Germany. E-mail: rne@mpe.mpg.de F. Comerón, European Southern Observatory, D-85748 Garching, Germany. E-mail: fcomeron@eso.org

between giant stars (where the Na I absorption lines are weaker) and dwarf stars (where the Na I lines are deeper), which indicates a surface gravity consistent with that of a young object far above the main sequence. Hence, this object is a member of the Cha I star-forming region. Also, the strength of the Hα emission line indicates a young age, because all main-sequence dwarf stars with spectral type M show Hα equivalent widths ≤ 1.5 nm (*15*). Visual comparison with spectra of late M dwarfs (*16*) shows that Cha Hα 1 has a spectral type M7 or later. The standard star most similar to our object is Gl 752 B with a spectral type M8 (*16*). A more quantitative classification obtained with different indices based on flux ratios (*15*, *17*) yields a spectral type M7.5 to M8. Recent estimates of the temperature of the stellar photosphere based on spectral type (*8*) depend on the match between observed spectral features and synthetic model atmospheres predicted for a given temperature, metallicity, and surface gravity. The latest spectral type considered in such calibrations is M6, which is best fitted with a temperature of 2700 K.

If we extrapolate a linear fit to those calibrations (*18*) to the spectral type of Cha Hα 1, we obtain 2600 K for M7.5 and 2500 K for M8. For objects far above the main sequence, such calibrations yield temperatures that are higher by ~100 K (*5*). Hence, it seems adequate to adopt 2700 K as the upper limit. Even allowing ±150 K uncertainty (*8*), this upper limit places Cha Hα 1 below 2900 K, the temperature of the most massive BD of its luminosity, which is constrained by the optical and NIR photometry (*7*). With a luminosity of 0.015 $L_\odot$, estimated from the photometry and visual extinction A_V (*7*), and an effective temperature of 2700 K, comparison with the new sets of evolutionary tracks (*10*) consistently yields an age of 10^6 years and a mass of 0.04 ± 0.01 $M_\odot$. Because the upper mass limit for BDs is 0.08 $M_\odot$, Cha Hα 1 can be classified as a BD.

Although low-mass objects are fully convective (*6*), convection alone is not enough to

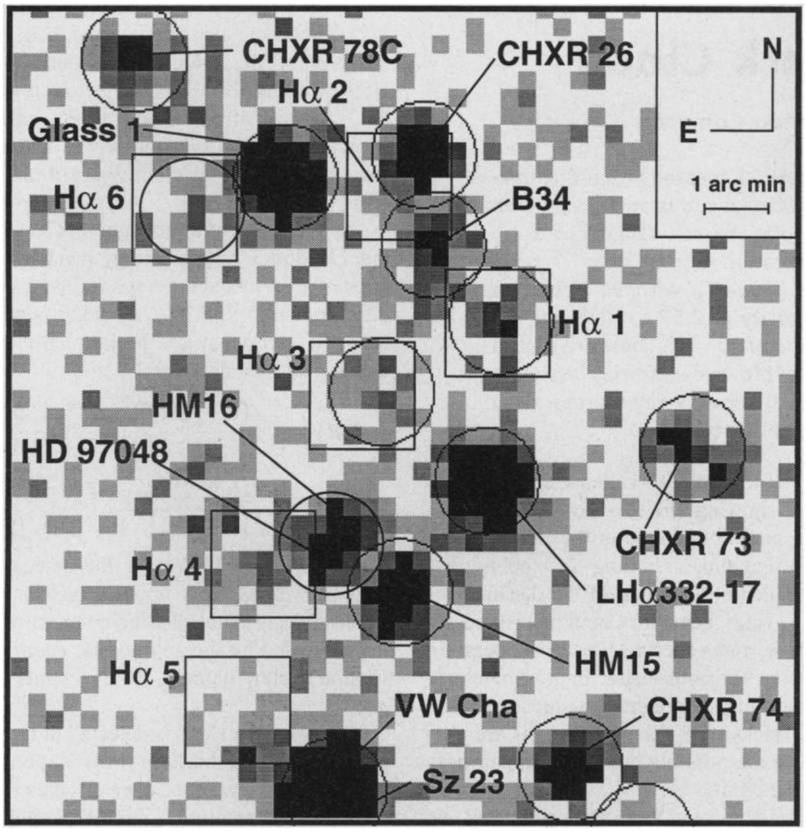

Fig. 1. Central part of the hard 0.5- to 2.1-keV band ROSAT PSPC image centered on the Cha I dark cloud with ROSAT sources detected above 3σ in the hard band as circles and other members of the Cha I cloud as squares.

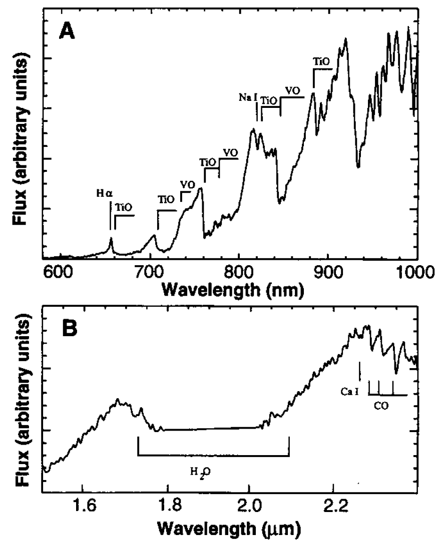

Fig. 2. (**A**) Visible and (**B**) infrared spectra of Cha Hα 1 obtained with the NTT in May 1998. The visible spectrum is ratioed by the instrumental throughput curve, so that the feature intensity ratios are preserved. The infrared spectrum was divided by that of a nearby F7V star observed immediately after Cha Hα 1 at the same air mass to remove telluric features. The flat portion of the spectrum between 1.79 and 2.02 μm is due to strong atmospheric absorption. The most relevant features identified are marked.

Table 1. X-ray data of very low mass members of the Cha I dark cloud: designation, optical position, spectral type, visual extinction A_V [all from (*7*), but spectral type of Cha Hα 1 from this work] (mag, magnitude), positional offset, significance of the detection (det. sgn.) in the hard band (0.5 to 2.1 keV) where the sources are detected most significantly, effective exposure time (exp.), hardness ratios, number of x-ray counts in the broad band (0.1 to 2.4 keV) either as detections or upper limits (both background subtracted), x-ray luminosity (at 160 pc), and ratio of x-ray to bolometric luminosity. NR, not resolved, 29 arc sec southeast of an x-ray source identified as CHXR 26 (*25*). ND, not detected.

Object designation	Optical position		Spectral type	A_V (mag)	Off-set	Det. sgn.	Exp. (ks)	Hardness ratios		X-ray counts	log (L_X) (erg/s)	log (L_X/L_{bol})
	α2000	δ2000						*HR*1	*HR*2			
Cha Hα 1	11 07 17.0	−77 35 54	M7.5-8	1.77	4″	9 σ	37.8	≥0.40	0.15 ± 0.22	31.4 ± 7.7	28.41 ± 0.10	−3.44
Cha Ha 2	11 07 43.0	−77 33 59	M6	3.55	NR	NR	37.8					
Cha Hα 3	11 07 52.9	−77 36 56	M6	2.13	17″	4 σ	37.6	≥0.13	0.04 ± 0.35	11.9 ± 5.7	27.99 ± 0.17	−4.31
Cha Hα 4	11 08 19.6	−77 39 17	M6.5	0.71	ND	ND	34.8	ND	ND	≤22.9	≤28.31	≤−4.91
Cha Hα 5	11 08 26.9	−77 41 21	M6	2.48	ND	ND	33.9	ND	ND	≤1.98	≤27.26	≤−5.24
Cha Hα 6	11 08 40.2	−77 34 17	M6	0.71	10″	4 σ	31.8	≥0.26	0.08 ± 0.40	8.2 ± 3.4	27.90 ± 0.15	−4.09

generate magnetic fields and coronal x-ray emission. A rotation-induced dynamo is needed (*6*). The star VB 8 with spectral type M7 is the star with the latest spectral type that shows quiescent x-ray emission, namely, log $(L_x/L_{bol}) = -2.8$ (where L_x is the x-ray luminosity and L_{bol} is the bolometric luminosity) (*19*). Also, the M8 star VB 10 was detected at log $(L_x/L_{bol}) \simeq -3$, but only during a flare. The quiescent upper limit is log $(L_x/L_{bol}) \leq -4.5$ before and after the flare (*20*). In addition, the M6 to M7 T Tauri star V410 x-ray 3 was also detected as an x-ray source (*21*). With a mass of 0.08 to 0.15 $M_\odot$, an age of 10^6 years, and log $(L_x/L_{bol}) = -2.8$ (*22*), it is similar to Cha Hα 1, but slightly more massive. The object 1623-2426, a young BD in ρ Oph (*5*), was not detected in the 33-ks PSPC pointed observation 200045, newly reduced by us (*23*), with the upper limit being log $(L_x/L_{bol}) \leq -3.26$, above the value measured for Cha Hα 1.

With an optical magnitude in the V band of 21 magnitudes (*7*), Cha Hα 1 is the optically faintest low-mass object we observed. Yet, it is the x-ray brightest object, and the x-ray to bolometric luminosity relation cannot explain why only Cha Hα 1 is detected in x-rays. It is possible that Cha Hα 1 rotates fast to support a strong dynamo. The spectral resolutions of our observations are too low to determine the rotational velocity. Because ρ Oph 1623-2426 has a mass similar to Cha Hα 1 and is 3 to 10 times older, but it is not detected as an x-ray source, only the combination of a young age ($\leq 3 \times 10^6$ years) and fast rotation (≥ 20 km/s) may allow us to detect x-ray emission from a BD (*24*). Alternative models for BD x-ray emission appear less likely: (i) Flare activity without (or with faint) quiescent emission, for example, due to magnetic field reconnections, as in the late-type star VB 10 (*20*), is not supported by our observations, because we find no evidence for variability in the x-ray emission. (ii) If Cha Hα 1 were a close binary with magnetic field configurations similar to those in x-ray bright, interacting low-mass binaries, it should be brighter in the optical than observed (*7*). (iii) The x-ray emission cannot be linked with any circumstellar material, because we do not see any NIR excess (*7*). Hence, coronal activity appears to be the most plausible explanation for the x-ray emission that is consistent with all the other observational data.

The x-ray detection of Cha Hα 1 suggests that a young BD can support a magnetic corona. Therefore, it may be possible to find more young BDs in star-forming regions as counterparts to faint x-ray sources in x-ray observations with long exposure times. Establishing the BD x-ray luminosity function and estimating the integrated x-ray emission are important for assessing the BD contribution to the diffuse galactic x-ray emission and the baryonic dark matter in the galactic halo.

References and Notes

1. A. Burrows and J. Liebert, *Rev. Mod. Phys.* **65**, 301 (1993); S. R. Kulkarni, *Science* **276**, 1350 (1997).
2. A. Burrows *et al.*, *Nature* **375**, 299 (1995).
3. J. R. Stauffer, D. Hamilton, R. Probst, *Astron. J.* **108**, 155 (1994); R. Rebolo, M. R. Zapatero-Osorio, E. L. Martín, *Nature* **377**, 129 (1995); G. Basri, G. W. Marcy, J. Graham, *Astrophys. J.* **458**, 600 (1996); M. R. Zapatero-Osorio, R. Rebolo, E. L. Martín, *Astron. Astrophys.* **317**, 164 (1997).
4. F. Comerón, G. H. Rieke, P. Claes, J. Torra, R. J. Laureijs, *Astron. Astrophys.* **335**, 522 (1998).
5. K. L. Luhman, J. Liebert, G. H. Rieke, *Astrophys. J.* **489**, L165 (1998).
6. B. Dorman, L. Nelson, W. Chau, *ibid.* **342**, 1003 (1989); F. D'Antona and I. Mazzitelli, *ibid.* **296**, 502 (1985).
7. F. Comerón, G. H. Rieke, R. Neuhäuser, in preparation.
8. S. K. Leggett, F. Allard, G. Berriman, C. C. Dahn, P. H. Hauschildt, *Astrophys. J. Suppl.* **104**, 117 (1996).
9. F. Allard, P. H. Hauschildt, D. R. Alexander, S. Starrfield, *Annu. Rev. Astron. Astrophys.* **35**, 137 (1997).
10. A. Burrows *et al.*, *Astrophys. J.* **491**, 856 (1997); F. D'Antona and I. Mazzitelli, in *Proceedings of the Meeting on Cool Stars in Clusters and Associations*, G. Micela, R. Pallavicini, S. Sciortino, Eds. (Astronomical Society of Italy, Florence, 1997), pp. 807–822; F. D'Antona *et al.*, in preparation; A. Burrows *et al.*, in preparation.
11. J. Trümper, *Adv. Space Res.* **2** (no. 4), 241 (1983); E. Pfeffermann *et al.*, *Proc. SPIE* **733**, 519 (1988).
12. E. D. Feigelson and G. A. Kriss, *Astrophys. J.* **338**, 262 (1989).
13. E. D. Feigelson *et al.*, *ibid.* **416**, 623 (1993).
14. M. Braun, thesis, Friedrich-Schiller Universität, Jena, Germany (1992).
15. J. Liebert *et al.*, in *7th Cambridge Workshop on Cool Stars, Stellar Systems, and the Sun*, vol. 26 of ASP Conference Series, M. S. Giampapa and J. A. Bookbinder, Eds. (ASP, San Francisco, 1992), pp. 282–283.
16. J. D. Kirkpatrick, T. J. Henry, D. W. McCarthy, *Astrophys. J. Suppl.* **77**, 417 (1991); J. D. Kirkpatrick, T. J. Henry, D. A. Simon, *Astron. J.* **109**, 797 (1995).
17. C. F. Prosser, J. R. Stauffer, R. P. Kraft, *Astron. J.* **101**, 1361 (1991); E. L. Martín, R. Rebolo, M. R. Zapatero-Osorio, *Astrophys. J.* **469**, 706 (1996).
18. K. L. Luhman and G. H. Rieke, *Astrophys. J.* **497**, 354 (1998).
19. M. S. Giampapa *et al.*, *ibid.* **463**, 707 (1996).
20. T. Fleming, J. H. M. M. Schmitt, M. S. Giampapa, in preparation.
21. K. M. Strom and S. E. Strom, *Astrophys. J.* **424**, 237 (1994).
22. K. L. Luhman *et al.*, *ibid.* **493**, 909 (1998).
23. A slightly larger x-ray upper limit was reported in (*5*) obtained from the 1σ noise level in the hard band ROSAT map published by S. Casanova *et al.* [*Astrophys. J.* **439**, 752 (1995)].
24. None of the 11 bona fide BDs published so far, all with ages $\geq 3 \times 10^6$ years and rotational velocities ≥ 20 km/s (as far as known), were detected in x-ray observations (R. Neuhäuser *et al.*, in preparation).
25. W. A. Lawson, E. D. Feigelson, D. P. Huenemoerder, *Mon. Not. R. Astron. Soc.* **280**, 1071 (1996).

26. We are grateful to H. Zinnecker, J. Schmitt, E. Martín, and G. Rieke for useful discussion about BDs, ESO for allocation of telescope time, C. Lidman and G. Carraro for allowing the use of their telescope time, A. Burrows and F. D'Antona for providing their new pre–main-sequence tracks, E. Feigelson for allowing the use of his ROSAT observation, the second processing of which is not yet publicly available, and B. Stelzer and T. Hearty for part of the specific software development. ROSAT is supported by the German government (BMBF/DLR) and the Max-Planck-Society.

6 July 1998; accepted 2 September 1998

Measuring the Spin Polarization of a Metal with a Superconducting Point Contact

R. J. Soulen Jr., J. M. Byers,* M. S. Osofsky, B. Nadgorny, T. Ambrose, S. F. Cheng, P. R. Broussard, C. T. Tanaka, J. Nowak, J. S. Moodera, A. Barry, J. M. D. Coey

A superconducting point contact is used to determine the spin polarization at the Fermi energy of several metals. Because the process of supercurrent conversion at a superconductor-metal interface (Andreev reflection) is limited by the minority spin population near the Fermi surface, the differential conductance of the point contact can reveal the spin polarization of the metal. This technique has been applied to a variety of metals where the spin polarization ranges from 35 to 90 percent: $Ni_{0.8}Fe_{0.2}$, Ni, Co, Fe, NiMnSb, $La_{0.7}Sr_{0.3}MnO_3$, and CrO_2.

A new class of electronics is emerging based on the ability of ferromagnetic metals to conduct spin-polarized currents (*1*). The effectiveness of magnetoelectronics depends on the extent to which a current is spin-polarized. All device designs improve their performance as the spin polarization $P \rightarrow 100\%$. For both scientific and technological reasons it is important to be able to directly and easily measure the electronic spin polarization at the Fermi energy, E_F, of a candidate material.

Unfortunately, determining P at E_F of a ferromagnet (FM) is not easy. A typical transition-metal FM has two components to its electronic structure: narrow d bands that may be fully or partially spin-polarized (due to the on-site exchange energy) and broad s bands with a lesser degree of spin polarization (due to hybridization with the d bands). The quantity P can be defined as

$$P = \frac{N_\uparrow(E_F) - N_\downarrow(E_F)}{N_\uparrow(E_F) + N_\downarrow(E_F)} \quad (1)$$

where $N_\sigma(E)$ is the spin-dependent density of states. The value of P is controlled by the